

# Decomposition of Azocumene on Silica Surfaces

J. E. Leffler\* and J. J. Zupancic

Contribution from the Department of Chemistry, Florida State University, Tallahassee, Florida 32306. Received April 5, 1979

**Abstract:** The decomposition of azocumene on silica surfaces in the absence of solvent is slower than in toluene solution and has a much lower radical efficiency. Radicals that escape geminate reaction can be trapped by adsorbed bis(diphenyl)phenylallyl. The ratio of cumene to  $\alpha,\alpha$ -dicumyl is about five times that in toluene. Aromatized  $\alpha$ -ortho and  $\alpha$ -para cumyl dimers, found only in the reactions on silica, are formed in low yield. These products (**10** and **11**) are formed via the quinoidal  $\alpha$ -ortho and  $\alpha$ -para dimers, which have been reported as transient products in toluene. The aromatized dimers (**10** and **11**) are exclusively geminate recombination products, presumably because they are formed only if the site at which the azocumene decomposes is also a catalytic site for the aromatization of the quinoidal dimers. The rates and product ratios depend to some extent on the purity and degree of hydroxylation of the silica. They also depend on the fraction of a monolayer occupied by the azocumene. At low monolayer coverages the azocumene is preferentially adsorbed on sites that give lower rates, higher cumene to  $\alpha,\alpha$ -dicumyl ratios, and higher yields of the aromatized dimers **10** and **11**. The silicas were characterized by their acidities,  $R_f$  values, catalytic properties, and the electron paramagnetic resonance spectra of adsorbed radicals.

Azocumene (**1**) is a two-bond initiator whose decomposition into cumyl radical pairs has been extensively studied for liquid solvents and glasses.<sup>1-3</sup> The available information includes rates, radical disproportionation/combination ratios, and the extent of geminate combination. The purpose of the research described in the present paper was to compare the liquid phase results with those for the reaction in the quite different medium offered by a silica surface. No solvents were present during the reaction stage of these experiments and the temperature was such that vapor phase reaction could be ignored.

The variables in our experiments were the surface analogue of concentration (monolayer fraction), the presence of adsorbates other than the azocumene, thermolysis at 55 °C vs. photolysis at 25 °C, the presence or absence of a stable radical scavenger, the purity of the silica, and the hydroxylated vs. dehydroxylated nature of the silica surface.

**Characteristics of the Surfaces and Adsorbates.** As a necessary preliminary to the discussion of the product and kinetic data, an abbreviated discussion of the surfaces is given at this point.<sup>4</sup> Four types of silica were used: a high purity silica designated here by  $P_1H_1$ , an otherwise similar silica of lower purity containing more Fe and Ti, designated as  $P_0H_1$ , and dehydroxylated samples of the same silicas,  $P_0H_0$  and  $P_1H_0$ . The dehydroxylated silicas were prepared by heating in vacuo at 850 °C for 10 h. This procedure is known to remove surface hydroxyl groups.<sup>5</sup> The resulting surface has lost its geminal and vicinal OH group clusters. What remains is mostly siloxane linkages and isolated rather than clustered OH groups;<sup>5</sup> it should also be noted that the change is irreversible and that nothing like the original surface can be regenerated by exposure to water vapor.<sup>5</sup>

Cumyl radicals are rotationally mobile but stable on the surface ( $P_0H_1$ ) as shown by the degree of resolution of the EPR hyperfine structure at -153 °C (Figure 1). At -129 °C the radical is translationally mobile as well and the signal decays with a half-life of about 1 h. In contrast, larger molecules such as 1,1,3,3-bisdiphenylene-2-phenylallyl (BDPA) are nearly immobile even at the temperature of our thermolysis experiments. The degree of resolution shown by this radical in ethanol at -113 °C suggests a  $\tau_{rot}$  greater than  $10^{-7}$  s; on a silica surface, the same degree of resolution is not reached until +185 °C (Figure 2). Adsorbed diphenyl nitroxide shows a nitrogen hyperfine triplet distorted by constraints on the rotation of the radical. At 55 °C,  $\tau_{rot}$ <sup>6-8a</sup> is about  $10^{-9}$  s on both of the  $H_1$  silicas and  $10^{-8}$  on the  $H_0$  silicas.

We also characterized the surfaces by their proton exchange or prototropic catalysis, by their shifts of the diphenyl nitroxide

$g$  value,<sup>10</sup> indicator acidity, and  $R_f$  values.<sup>9</sup> The results of both the EPR and the other experiments can be summarized as follows: A higher level of purity ( $P_1$ ) goes with lesser acidity, lesser catalytic activity, and slightly greater adsorbate mobility. A higher level of hydroxylation ( $H_1$ ) goes with greater mobility of adsorbed molecules or radicals and with a somewhat greater acidity.

**Kinetics.** Reactions on surfaces will almost always differ in their kinetics from otherwise similar reactions in liquid solvents. In liquids, although the nominal reagent is in fact a mixture of variously solvated subspecies, the reagent nevertheless behaves as a single *chemical species*<sup>11</sup> because the equilibria among the solvation subspecies are rapid. A similar neglect of the fundamental complexity of an adsorbed reagent is usually not possible. Unlike solvent molecules, the various surface microenvironments are immobile, and the mobility of the adsorbed reagent is also limited. Thus the decomposition of azocumene, though essentially a simple unimolecular process, gives first-order plots that are concave down (Figure 3). Motions on the surface are too slow to repopulate the faster decomposing subspecies while they are being depleted by the main reaction.

In the present reaction, the subspecies are enough alike, however, so that the rate constants from the first two half-lives or so provide a useful basis for discussion.

**Site Discrimination.** As can be seen from Figure 4, the approximate first-order rate constants depend on the initial fraction of the surface occupied by the azocumene. The rate constants at first increase rapidly with monolayer fraction and then level off. This can be most readily explained if the azocumene has been preferentially adsorbed on a minority of silica gel sites corresponding to the slower decomposing subspecies. It will be convenient to call these S sites. At higher fractions of monolayer coverage, the S sites are filled and the additional azocumene begins to occupy sites that correspond to faster decomposing subspecies. Apparently most of the sites belong to the faster subspecies and these do not differ greatly among themselves.

**Site Preemption.** Other compounds adsorbed on the silica S sites can prevent in part their occupation by the azocumene, again causing the rate constants to be higher. For an azocumene monolayer fraction of about 0.019 on  $P_0H_1$  silica, applying about the same amount of azobenzene after the azocumene increased the rate constant by about 7%; a similar experiment, in which the azobenzene was put on before the azocumene, increased the rate constant by about 15%. Putting BDPA radical on  $P_0H_0$  silica after the azocumene increased the rate constant about 10%, put on before, by about 15%. Rate

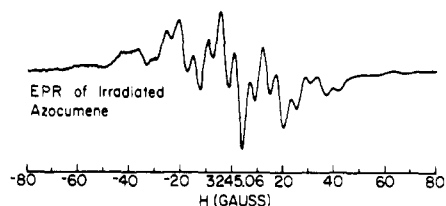


**Figure 1.** 9-GHz EPR spectrum of cumyl radicals from the photolysis of azocumene adsorbed on  $P_0H_1$  silica, photolyzed at  $-196^\circ\text{C}$ , observed at  $-153^\circ\text{C}$ . The  $g$  value is 2.0026 and the  $\beta$ -H hyperfine constant is 16.6 G.

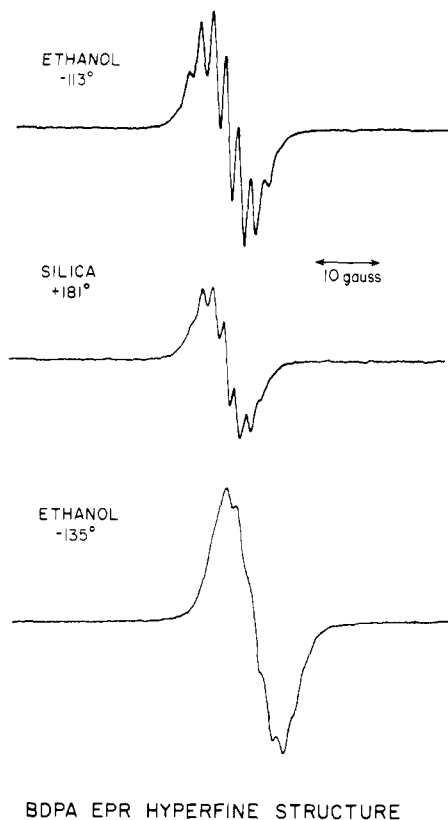


**Figure 2.** Comparative behavior of BDPA in ethanol and on silica.

constants measured by the fading of the BDPA EPR signal on the various silicas were on the average about 4% greater than those obtained in the absence of BDPA using nitrogen evolution to follow the reaction.

**Medium Effects and the Nature of the Slow Sites.** Table I compares rate and activation parameters for two of the silica surfaces with those for toluene<sup>1</sup> solution. The rate has also been measured in benzene–thiophenol, where the decomposition is somewhat faster than it is in toluene.<sup>1</sup> Although nothing can be said about the relative importance of enthalpy and entropy contributions to the rate differences between the various silicas, the higher rate in toluene than on the silicas may be due to a more favorable entropy of activation.

The interaction of the azo compound with the slow surface sites (S sites) most probably involves geminal or vicinal hydroxyl groups,<sup>12–15a</sup> since the dehydroxylation, which leaves mainly isolated hydroxyl groups,<sup>5</sup> gives a surface on which the proportion of slow sites is less and the rates are greater. The fact that the decomposition rates are also lower on the more acidic, better hydrogen bonding  $P_0H_1$  silica than on  $P_1H_1$  silica also indicates that the important interaction with the surface is hydrogen bonding.<sup>14,15a</sup> A similar conclusion was reached by Leermakers et al. in their study of the electronic spectra of adsorbed azo compounds.<sup>15b</sup> We do not attribute the lower

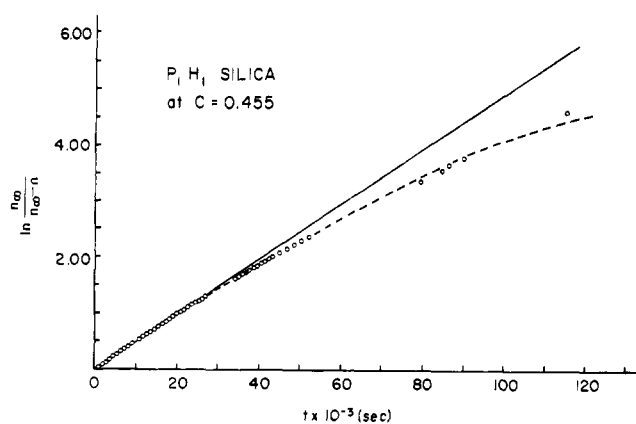


**Figure 3.** Kinetics of nitrogen evolution;  $k = 4.83 \times 10^{-5} \text{ s}^{-1}$ .

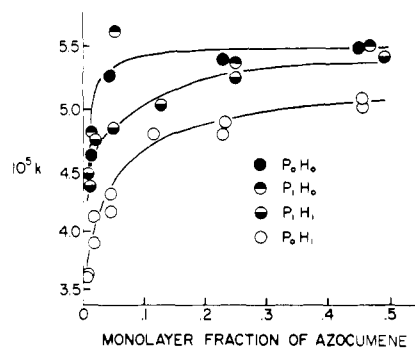


**Figure 4.** Effect of monolayer fraction and type of silica on the first-order decomposition rate constants. The independent variables are  $P_0$  and  $P_1$ , low and high purity silica,  $H_0$  and  $H_1$ , low and high density of surface OH groups.

**Table I**

medium	$10^5 k$ ( $55^\circ\text{C}$ ), $\text{s}^{-1}$	$\Delta H^\ddagger$ , kcal/mol	$\Delta S^\ddagger$ , cal/(mol deg)
toluene	8.8 <sup>a</sup>	29.1 <sup>a</sup>	11.3 <sup>a</sup>
$P_1H_1$ silica <sup>b</sup>	4.7	29.0 <sub>5</sub> <sup>c</sup>	10.0 <sup>c</sup>
$P_0H_1$ <sup>b</sup>	3.9	29.2 <sup>c</sup>	10.2 <sup>c</sup>
$P_1H_0$ <sup>b</sup>	5.0		
$P_0H_0$ <sup>b</sup>	5.0		

<sup>a</sup> Calculated from best Arrhenius parameters, ref 1, temperature range  $40$ – $69^\circ\text{C}$ . <sup>b</sup> For 0.02 of a monolayer. <sup>c</sup> Temperature range  $35$ – $65^\circ\text{C}$ .

rates on  $P_0H_1$  to any direct interaction with impurity atoms since the level of impurities is quite low.

**Products.** The products from the decomposition of azocumene on silica are shown in reactions 1–4 and 7, and the yields for the various conditions are given in Table II. Cumene (3),  $\alpha$ -methylstyrene (2), and dicumyl (4) are also formed in liquid, solid, or glassy media, but with major differences in the relative yields.<sup>1,2</sup> The ratio of the rate of disproportionation to that of radical combination is usually estimated from the cumene/dicumyl yield ratio. As in the present experiments,  $\alpha$ -methylstyrene yields tend to be lower than cumene yields because of subsequent reactions of the  $\alpha$ -methylstyrene, not all of which give readily isolable products.

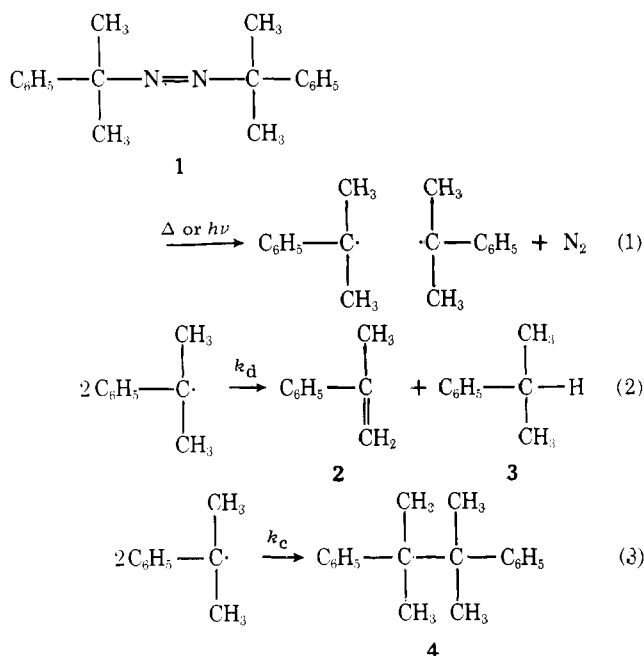
**Disproportionation vs. Coupling.** In liquid benzene solution,  $k_d/k_c$  of the cumyl radicals from azocumene is  $0.055 \pm 0.005$  and does not appear to be correlated with the thermolysis temperature or with photolysis vs. thermolysis of the azo compound.<sup>1</sup> The effects of changes in the azo compound or in the fluid vs. solid nature of the medium are large, however. Thus photolysis of 2,2'-azoisobutane in liquid benzene is re-

Table II<sup>a,b</sup>

product and anal. precision <sup>c</sup>		C <sub>0</sub> P <sub>0</sub> H <sub>1</sub> <sup>a</sup>	C <sub>1</sub> P <sub>0</sub> H <sub>1</sub>	C <sub>0</sub> P <sub>1</sub> H <sub>1</sub>	C <sub>1</sub> P <sub>1</sub> H <sub>1</sub>	C <sub>0</sub> P <sub>0</sub> H <sub>0</sub>	C <sub>1</sub> P <sub>0</sub> H <sub>0</sub>	C <sub>0</sub> P <sub>1</sub> H <sub>0</sub>	C <sub>1</sub> P <sub>1</sub> H <sub>0</sub>
cumene ± 0.0038	T <sub>0</sub>	0.1166 <sup>b,d</sup>		0.0981 <sup>d</sup>		0.0965 <sup>d</sup>		0.0707 <sup>d</sup>	
	T <sub>1</sub>	0.0967	0.1182	0.0911	0.0872	0.1329 <sup>d</sup>	0.0871	0.0971	0.0719
α-Me-styrene ± 0.0025	T <sub>0</sub>	0.0235 <sup>d</sup>		0.0928 <sup>d</sup>		0.0403 <sup>d</sup>		0.0586 <sup>d</sup>	
	T <sub>1</sub>	0.0260	0.0106	0.0739	0.0689	0.0197 <sup>d</sup>	0.0458	0.0940	0.0594
1,3,3-trimethyl-3-phenylindan ± 0.0021	T <sub>0</sub>	0 <sup>d</sup>		0 <sup>d</sup>		0.0212 <sup>d</sup>		0 <sup>d</sup>	
	T <sub>1</sub>	0.0152	0.0303 <sup>d</sup>	0	0	0.104 <sup>d</sup>	0.0114	0	0
aromatized head-to-tail dimers <b>10</b> & <b>11</b> ± 0.0056	T <sub>0</sub>	0.0575 <sup>d</sup>		0.0209 <sup>d</sup>		0.0425 <sup>d</sup>		0.0253 <sup>d</sup>	
	T <sub>1</sub>	0.0640	0.0484	0.0532	0.0415	0.0566	0.0406	0.0620	0.0497
dicumyl ± 0.0171	T <sub>0</sub>	0.5827 <sup>d</sup>		0.6614 <sup>d</sup>		0.6040 <sup>d</sup>		0.7322 <sup>d</sup>	
	T <sub>1</sub>	0.6877	0.7399	0.7052	0.7547	0.5567	0.7472	0.6594	0.7801

<sup>a</sup> Explanation of reaction conditions. C<sub>0</sub> ≈ 0.02 monolayer fraction; C<sub>1</sub>, 0.4–0.5 monolayer fraction; P<sub>0</sub>, lower purity silica; P<sub>1</sub>, higher purity silica; H<sub>1</sub>, not dehydroxylated; H<sub>0</sub>, dehydroxylated; T<sub>0</sub>, photolysis at 25 °C; T<sub>1</sub>, thermolysis at 55 °C. <sup>b</sup> Yields are fraction of the azocumene cumyl moieties recovered in the form of that product. Unless otherwise noted, they are the mean values from two runs. <sup>c</sup> Estimate of standard deviation of a single measurement from pairs of replicate runs, four to eight pairs. Note that most of the entries in the table are the mean result of replicate runs. <sup>d</sup> A single run.

ported to give a  $k_d/k_c$  of 4.5.<sup>1</sup> And in frozen toluene, photolysis of azocumene gave ratios ranging from 1.5 to 3.<sup>1</sup> The effect of cage vs. noncage reaction is small; in the presence of a rad-



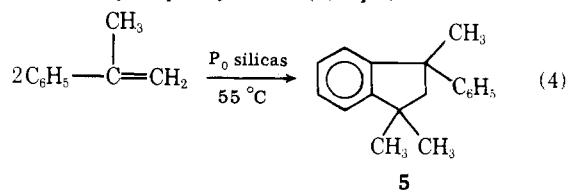
ical scavenger, the ratio for azocumene in liquid toluene was 0.066, or only about two standard deviations greater than that reported for the unscavenged reactions in benzene.<sup>2</sup>

On silica surfaces,  $k_d/k_c$  as measured by the cumene to dicumyl yield ratio had a mean value of 0.28. This number is an average over all four independent variables and two levels; its standard deviation of 0.07 represents the dispersion caused by different combinations of variables and levels. An analysis of the variance showed that the only variables of major significance in determining the value of  $k_d/k_c$  were the fraction of monolayer (C) coverage and the purity of the silica. The mean for the set of experiments having in common a C<sub>0</sub> level (~0.02) of monolayer coverage is 34% greater than the mean for the C<sub>1</sub> (~0.4) experiments. Similarly, the mean for the P<sub>0</sub> set is 32% greater than that for the P<sub>1</sub> set, and the mean for the set in which both C and P are at the lower level is 71% greater than for the C<sub>1</sub>P<sub>1</sub> set.

It may be recalled that low surface area coverage and low silica purity were both associated with a lower rate of decomposition of the azocumene (Figure 4). We interpreted this in terms of greater stabilization of a more strongly adsorbed azocumene on the minority sites and on the less pure silica. Putting all of the observations of  $k_d/k_c$  values together leads to the following generalization: constraints on the motion of the azocumene, and inferentially on the motion of the cumyl radicals as well, almost always increase the relative amount of disproportionation. This is the case whether the constraint is a glassy solvent, adsorption on a surface, adsorption on a more strongly adsorbing surface, or adsorption on a more strongly adsorbing site (S site) of a given surface. However, the motional constraint expected for H<sub>0</sub> surfaces appears to be an exception.

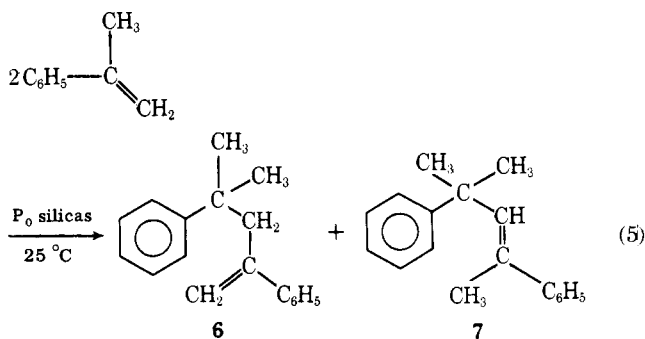
The effect of motional constraints can be most easily explained if the activation energy for coupling of the radical pair is slightly less than that for disproportionation. As was pointed out by Nelsen and Bartlett,<sup>1</sup> there are more orientations of the radical pair suitable for disproportionation than for coupling. A less constrained radical pair has a better chance of achieving one of the scarcer orientations favoring coupling before reaction takes place. The coupling reaction rate is rotationally diffusion controlled as well as translationally diffusion controlled. The question of cage or geminate vs. nongeminate  $k_d/k_c$  can now be reexamined. The slightly higher (+ two standard deviations) value for the geminate  $k_d/k_c$  is in the expected direction for a more constrained radical pair.

**Dimers of α-Methylstyrene.** The yield of α-methylstyrene on silica is always less than the cumene yield, because the α-methylstyrene is subject to further reactions. On the P<sub>0</sub> silicas the major loss of α-methylstyrene is due to its conversion into 1,1,3-trimethyl-3-phenylindan (**5**, eq 4). This was con-

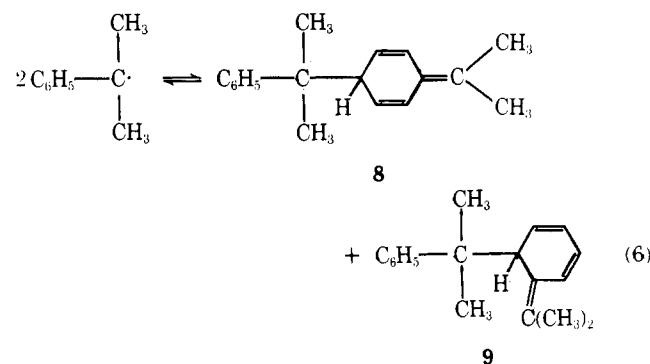


firmed by control experiments with the styrene by itself on P<sub>0</sub> silicas at 55 °C. Reaction 4 has also been reported to occur on zeolites.<sup>16</sup> Control experiments at 25 °C on P<sub>0</sub> silicas gave only the open chain dimers **6** and **7**. The formation of **5** was observed in one photolysis of the azocumene on a P<sub>0</sub> silica at 25 °C, but

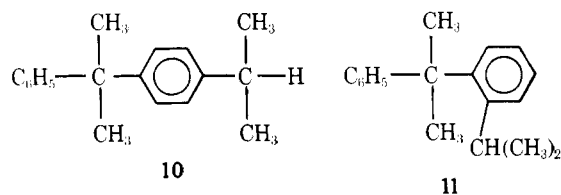
this was not further investigated. No **5** was formed on any P<sub>1</sub> silica under any conditions.



**Head-to-Tail Cumyl Dimers.** Photolysis of azocumene in solution at low temperatures is reported to give the dimers **8** and **9**, which were spectroscopically identifiable, although they could not be isolated.<sup>1,16b</sup> On standing the dimers disappeared from the solution by dissociation (eq 6) made irreversible by



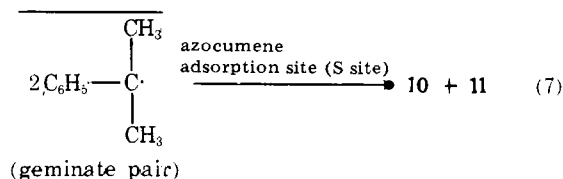
subsequent coupling and disproportionation reactions. The dissociation reaction is reported to have an enthalpy of activation of about 26 kcal/mol and an entropy of activation of about 11 eu. No traces of the *aromatized* dimers **10** and **11**



could be detected in the products from the solution experiments.<sup>1</sup> It was also noted that the addition of pyridine or of HCl in ether failed to accelerate the disappearance of **8** and **9** from solution; apparently prototropy is unable to compete with the dissociation reaction even under these conditions.<sup>1</sup>

The results on silica were quite different; **10** and **11** were formed from decomposing azocumene on all of the silicas under all conditions (Table II). The ratio of compound **11** to **10** in the mixture of these two products was about 3:1 based on the relative intensities of the methyl group signals in the decoupled <sup>13</sup>C magnetic resonance spectrum. Control experiments established that **10** and **11** were not formed from cumene or  $\alpha$ -methylstyrene or from both together on the silica.

Experiments with isotopically labeled azocumene, to be described later in connection with geminate and nongeminate reaction, established that **10** and **11** are *exclusively products of the geminate reaction*:



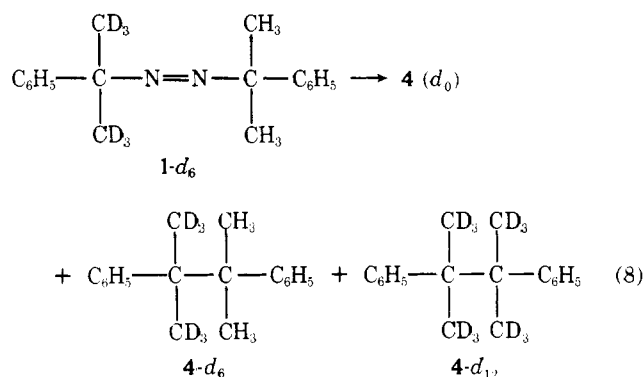
The most probable explanation for this is that the S sites, at which the azocumene is preferentially adsorbed, are also catalysts for aromatization of the head-to-tail dimers. Nongeminate dimers are no doubt formed elsewhere but do not encounter an S site before dissociating.

As expected on the basis of the above model, the yield of **10** plus **11** is greater in experiments where the S sites accommodate a larger fraction of the adsorbed azocumene. Thus the yield from the C<sub>0</sub>T<sub>1</sub> experiments was 31% greater than that from the C<sub>1</sub>T<sub>1</sub> set, and the yield from the P<sub>0</sub> set was 23% greater than that from the set of all experiments at the P<sub>1</sub> level of silica purity. The photolysis experiments also gave more of the aromatized dimers than the thermolysis experiments; the yield from the T<sub>0</sub>C<sub>0</sub> set exceeded that from the T<sub>1</sub>C<sub>0</sub> set by 23%. We did not determine whether this was due to a photoaromatization or merely to the longer residence time of the geminate pair on the active site at the lower temperature.

**The Radical Efficiency.** In toluene at 55 °C the radical efficiency (*f*) as determined by means of scavengers is about 75%. On silica, in contrast, BDPA is able to trap only 10–20% of the radicals, the rest giving geminate reaction products.

Of several scavengers tested on silica, only BDPA proved to be suitable.<sup>17</sup> The yield of nongeminately reacting radicals was measured by the fading of the BDPA EPR signal in situ on the silica. The completeness of trapping was tested by varying the BDPA monolayer fraction. In the range of 0.16 × 10<sup>-2</sup> to 0.75 × 10<sup>-2</sup> of a BDPA monolayer on P<sub>0</sub>H<sub>0</sub>, *f* in 12 experiments had a mean value of 0.132 ± 0.013 and the variation appeared to be random, suggesting that the trapping was complete. However, three experiments at 2.55 × 10<sup>-2</sup> of a BDPA monolayer gave *f* = 0.173 ± 0.003. Perhaps BDPA at this high monolayer fraction preempts sites at which the azocumene would otherwise have given lower radical efficiencies.

As a byproduct of experiments with the unsymmetrically deuterated azocumene **1-d<sub>6</sub>**, it is possible to make approximate estimates of *f* to supplement the scavenger results. In the absence of geminate recombination and of kinetic isotope effects, **1-d<sub>6</sub>** would give **4 (d<sub>0</sub>)**, **4-d<sub>6</sub>**, and **4-d<sub>12</sub>** in the statistical ratio



1:2:1. With geminate recombination, but without kinetic isotope effects, the product ratios and the radical efficiency would be related by eq 9.

In eq 9, *d<sub>0</sub>*, *d<sub>6</sub>*, and *d<sub>12</sub>* represent the relative yields of the corresponding isotopic dicumyls.

$$(d_0 + d_{12}) / (d_6) = f / (2 - f) \quad (9)$$

However, because part of the reaction occurring within the "cage" is subject to a primary isotope effect, the yield of escaped radicals must be somewhat increased by the deuterium labeling. This effect can be seen in Table III. There will also be some changes in the relative dicumyl yields because of the lesser tendency of deuterated radicals to disproportionate rather than couple. The yields of the isotopic dicumyls in the unresolved mixture of all four were estimated from the inten-

Table III. Radical Efficiencies  $f$ 

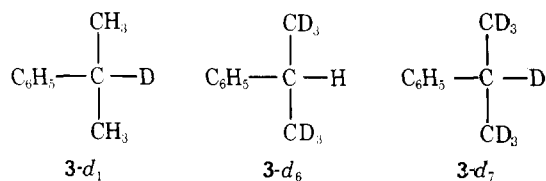
reaction conditions <sup>a</sup>	$f$ from scavenger azocumene <b>1</b>	BDPA monolayer fraction <sup>d</sup>	$f$ from product ratio eq 9 azocumene- $d_6$
toluene "gas", 200 °C <sup>c</sup>	0.75 <sup>b</sup>		0.78
neat, melting 86 °C			0.86
			0.48
P <sub>0</sub> H <sub>1</sub> C <sub>0</sub> <sup>a,e</sup>	0.17	0.0255	0.18
	0.132 ± 0.013	0.0016–0.0075	
P <sub>1</sub> H <sub>1</sub> C <sub>0</sub>	0.132 ± 0.015	0.0086	0.19
	0.10	0.0027	

<sup>a</sup> Thermolysis. Temperature 55 °C except where otherwise noted. At low monolayer fractions: for the azocumene experiments, C<sub>0</sub> = 0.019–0.021; for the azocumene- $d_6$  experiments, 0.012–0.014. <sup>b</sup> From Nelsen and Bartlett.<sup>2</sup> <sup>c</sup> A benzene solution of 1- $d_6$  was injected into the inlet port of the GLC held at 200 °C. There may be some condensed phase or wall reaction. <sup>d</sup> Present in the experiments with azocumene **1** only. <sup>e</sup> See Table II footnotes for variables P and H and levels 0 and 1.

sities of peaks in the chemical ionization mass spectrum corresponding to the dicumyls minus one phenyl group.<sup>19</sup>

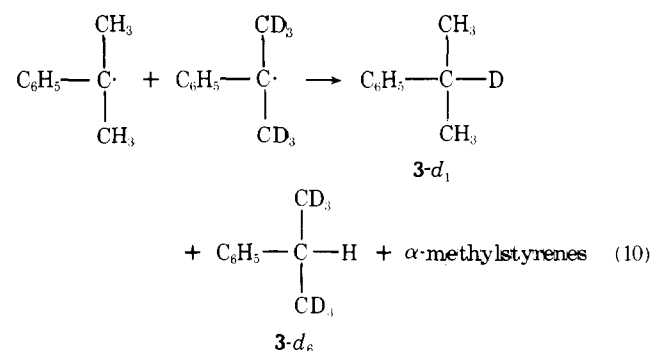
A molecule adsorbed at an isolated hydrogen bond donor site should diffuse less readily than it would on a surface with many such sites close together.<sup>20</sup> The data in Table IV are in accord with this diffusion principle. Thus in all instances but one, the radical efficiency is lower on dehydroxylated silica, and the apparent exception is a photolysis in which  $f$  is already low because of the lower temperature. Covering part of the surface with azobenzene also decreases  $f$  (Table IV), possibly because adsorbed azobenzene blocks part of the hydroxyl-rich diffusion paths.<sup>21</sup>

**The Distribution of Hydrogen and Deuterium.** Control experiments with cumene- $d_7$  (3- $d_7$ ) on P<sub>0</sub> and P<sub>1</sub> silicas at 55 °C gave no exchange of D for H. In addition, the cumene formed by the thermolysis of azocumene on partly deuterated P<sub>0</sub> or P<sub>1</sub> silica contained no deuterium. The cumene from the decomposition of 1- $d_6$ , either thermally at 55 °C or photochemically at 25 °C, on all four undeuterated silicas (P<sub>0</sub> or 1-H<sub>0</sub> or 1) consisted exclusively of the isotopic species 3( $d_0$ ), 3- $d_1$ ,



3- $d_6$ , and 3- $d_7$ . Hence, neither cumene nor cumyl radicals exchange hydrogen with the surface.

The combined primary and secondary isotope effect for reaction 10 can be obtained from the 3- $d_6$ /3- $d_1$  product ratio.

Table IV. Radical Efficiencies for 1- $d_6$ 

reaction conditions <sup>a,b</sup>	T <sub>1</sub> <sup>a</sup> C <sub>0</sub> <sup>b</sup>	T <sub>1</sub> <sup>a</sup> C <sub>1</sub> <sup>e</sup>	C <sub>0</sub> <sup>b</sup> T <sub>1</sub> AZB <sup>d</sup>	T <sub>0</sub> <sup>a</sup> C <sub>0</sub> <sup>b</sup>
H <sub>1</sub> P <sub>0</sub>	0.18 (0.13) <sup>c</sup>	0.20	0.11 (0.0253) <sup>d</sup>	0.11
P <sub>1</sub>	0.19 (0.13) <sup>c</sup>	0.20	0.13 (0.0263) <sup>d</sup>	0.16
H <sub>0</sub> P <sub>0</sub>	0.10	0.15		0.13
P <sub>1</sub>	0.14	0.14		0.11

<sup>a</sup> See footnotes for Table II for meaning of variables PHT and levels 0 and 1. T<sub>0</sub> represents photolysis at 25 °C. <sup>b</sup> Experiments at relatively low 1- $d_6$  monolayer fractions, 0.011–0.014. <sup>c</sup> Parentheses contain data for **1**, not 1- $d_6$ , derived from scavenger experiments. <sup>d</sup> AZB is azobenzene, number in parentheses is AZB monolayer fraction. <sup>e</sup> Experiments at high monolayer fractions, 0.42–0.47.

Table V

composition, % dry basis	P <sub>0</sub> H <sub>1</sub> <sup>a,b</sup>	P <sub>1</sub> H <sub>1</sub> <sup>a,c</sup>
silica as SiO <sub>2</sub>	99.71	99.85
iron as Fe <sub>2</sub> O <sub>3</sub>	0.03	0.005
sodium as Na <sub>2</sub> O	0.02	0.004
calcium as CaO	0.02	0.018
titanium as TiO <sub>2</sub>	0.09	0.058
zirconium as ZrO <sub>2</sub>	0.03	0.030
characteristics		
pore vol, cm <sup>3</sup> /g	0.45	0.4
mean pore diameter, Å	22	25–27
surface area, m <sup>2</sup> /g	750	700
volatile at 1750 F	6%	6.5%
mesh size	28–200	100–200

<sup>a</sup> From Grace Davison Bulletin. <sup>b</sup> Fisher S-157, Grace Davison grade 12, lot no. 753475. <sup>c</sup> Fisher S-679, Grace Davison grade 923, code no. 9230808226.

It is 2.23 in toluene and not significantly different for the reaction on silica.

The low value of the isotope ratio for reaction 10 is compatible with a radical-like transition state in which the bond distance is too great for tunneling to be important.<sup>22</sup>

The  $\alpha$ -methylstyrenes are formed by four different reactions, each with a different isotope effect. In addition each  $\alpha$ -methylstyrene is subject to isotopic exchange with the silica, and on low purity silica, to dimerization reactions. The resulting isotopic mixtures contain species with from zero to five deuterium atoms.

The aromatized head-to-tail dimers **10** and **11** formed by the decomposition of 1- $d_6$  on the silicas all have precisely the six deuterium atoms required by an exclusively geminate reaction. The decomposition of the undeuterated azocumene **1** on partially deuterated P<sub>0</sub>H<sub>1</sub> or P<sub>1</sub>H<sub>0</sub> silica gives **10** and **11** in which only the methine hydrogen position contains some deuterium. This is as expected if **10** and **11** are formed from the quinoidal dimers by addition and removal of a proton. The lower yield of **10** and **11** on the deuterated silicas is also to be expected if the rate-determining step involves transfer of a proton from the surface to the methine position.

## Experimental Section

**Silicas.** The silica gels (Table V) were made by W. R. Grace and Co., Davison Chemical Division, and obtained through the Fisher Scientific Co. The silica was stored in a drying oven at 85 °C before use.

**Dehydroxylated Silica Gels (H<sub>0</sub>).** Ten to eleven grams of P<sub>0</sub> or P<sub>1</sub>H<sub>1</sub> silica was placed in a Vycor tube and outgassed at room temperature. It was then slowly heated between 750 and 850 °C at 10<sup>-5</sup> mm and, on attaining the upper temperature, held there for a total of 10 h. It was then sealed under vacuum and allowed to cool.

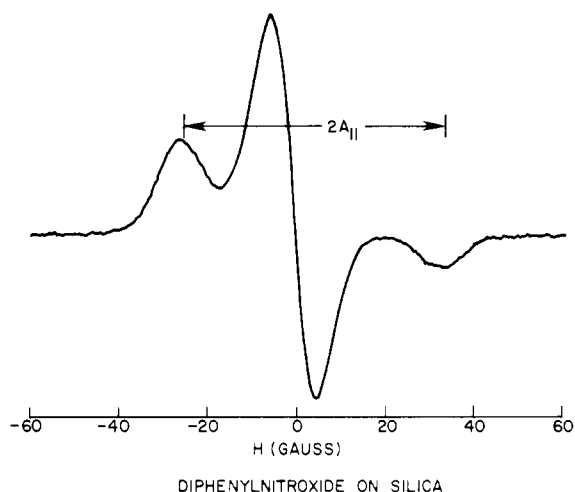


Figure 5. A .

**Deuterated Silica Gels.** Ten grams of  $P_0H_1$  or  $P_1H_1$  silica was allowed to stand for 3 days in contact with 25 mL of  $D_2O$  ( $\geq 99.8\%$  D) in a stoppered flask. Before use it was filtered and outgassed at  $10^{-3}$  mm until it was free flowing.

**A Comparison of Catalytic Activities.** Samples of 1,1,3,3,3-penta-deuterio-2-phenylpropene were adsorbed on  $P_1H_1$  and  $P_0H_1$  silicas at 0.11–0.14 monolayer fraction. The mass spectral intensities before and after heating were as follows:

	<i>m/e</i>					
	118	119	120	121	122	123
original material	0.24	0.66	0.74	1.00	0.96	0.66
90 h at 55 °C on $P_1H_1$	0.24	0.69	0.55	1.00	0.55	0.66
90 h at 55 °C on $P_0H_1$	0.27	1.00	0.23	0.24	0.08	0.06
90 h at 25 °C on $P_0H_1$	0.79	1.00	0.70	0.56	0.38	0.26

It should be noted that at 25 °C the propene was partly converted into exchanged open-chain dimers **6** and **7**, and at 55 °C into the cyclic dimer **5**.

**Adsorbed *p*-Dimethylaminoazobenzene.** In water this indicator changes from red to yellow in the pH range 2.9–4.0. On  $P_0H_1$  and  $P_0H_0$  it is red, on  $P_1H_0$  reddish yellow, and on  $P_1H_1$  yellow. The  $R_f$  values for the indicator developed with benzene<sup>9</sup> were 0.59 for  $P_1H_1$  (this corresponds to Brockmann activity grade II), 0.40 for  $P_0H_1$  (I), 0.31 for  $P_1H_0$  (I), and 0.19 for  $P_0H_0$  (I).

**Adsorbed Diphenyl Nitroxide.** In liquid solution the  $g$  value of diphenyl nitroxide has been correlated with the ability of the solvent to form hydrogen bonds.<sup>10</sup> For example,  $g$  is reported to be 2.0057 in  $CCl_4$ , 2.0055 in methanol, and 2.0051 in water. For diphenyl nitroxide on silica the apparent  $g$  value is lower than the true one because of a second effect of adsorption. The hindrance to motion on the surface broadens the high- and low-field components of the nitrogen hyperfine triplet to different extents, and since these partially overlap the center line the apparent position of the latter and the  $g$  value will change on the surface even if the mode of attachment does not involve a hydrogen bond. In any case, the lowered  $g$  values on our silica surfaces indicate strong adsorption forces.

The  $g$  value for diphenyl nitroxide adsorbed on  $P_1H_1$  silica at 25 °C was 2.0047 (apparent), on  $P_1H_0$  it was 2.0042, and on  $P_0H_0$  it was 2.0039, indicating a sequence of increasing acidity and/or hindrance to motion.

The behavior of the same radical on  $P_0H_1$  silica was more complicated. When this radical was initially adsorbed at room temperature, the  $g$  value was nearly the same as that on  $P_1H_1$  silica. However, on brief warming to 49 °C, the  $g$  value decreased irreversibly by about 0.0009. The rotational relaxation time as judged from the asymmetry of the spectrum did not seem to be affected by the warming, and the radical washed from the surface had the normal solution spectrum.

In principle it is possible to estimate  $\tau_{rot}$  for the adsorbed diphenyl nitroxide radical from the nitrogen hyperfine constant  $A_{||}$  (Figure 5).<sup>8a,b</sup> In practice, our line widths are too great for the results to be accurate, and the method also assumes that the  $g$  tensor components themselves do not change. At 55 °C  $\tau_{rot}$  by this method was about  $2.0 \times 10^{-9}$  s for the radical on  $P_1H_1$  silica, about the same ( $2.7 \times 10^{-9}$ )

on  $P_0H_1$ , but  $21 \times 10^{-9}$  on  $P_1H_0$  and  $12 \times 10^{-9}$  on  $P_0H_0$ . The activation energies for the rotations appeared to be about 5 kcal/mol, with the longer relaxation times on the dehydroxylated silicas due mainly to a lower preexponential factor. It may be that rotation of this radical is slower on the dehydroxylated silica because it is coupled with translation, a process that is facilitated by a continuous path of hydroxyl groups.

**Adsorbed BDPA.** The EPR spectrum of 1,1,3,3-bisdiphenylene-2-phenylallyl on  $P_0H_1$  silica (Figure 2) showed steadily increasing resolution of the hyperfine splitting as the temperature was raised from  $-196$  to  $+180$  °C. Apparently the motion remains in the slow range even at the highest temperature reached.<sup>6,7</sup> Similar experiments with ethanol solutions gave maximum resolution at  $-40$  °C and the resolution decreased at higher temperatures. The  $g$  value was 2.0025 on silica, in the crystalline radical and in solution.

**Adsorption Techniques: Slurry Filtration (SF).** This was used when a low monolayer fraction of a single compound was wanted. A slight excess of *n*-hexane was added to a weighed sample of the silica in a 250-mL flask to form a slurry. The compound to be adsorbed was then added in hexane solution, unless it was insoluble in that solvent. The slurry was stirred for 15 min, filtered by suction, and washed with hexane. When the silica was dry (no longer forming a solid cake), it was outgassed in the reaction vessel. The amount of nonadsorbed material (ordinarily zero) was estimated by UV examination of the filtrate and washings.

**Slurry Evaporation (SE).** In this variation on the SF technique, the solution of the compound to be adsorbed was added to the silica-hexane slurry in an indented round-bottomed flask and the solvent removed by tumbling in vacuo. After removal of the solvent, a small amount of *n*-hexane was added to form a slurry and the solvent again removed by tumbling in vacuo until the silica was free flowing. If a second compound was to be adsorbed, the silica was wet with a small amount of *n*-hexane, the solution of the second compound was added, and the previous manipulations were repeated. The silica was then transferred to the reaction vessel and outgassed.

The silica was protected from light during preparation, outgassing, and thermolysis.

**Monolayer Fraction, *C*.**  $C$  was calculated from the molecular area measured from models placed so as to lie as flat as possible, and this area divided by the area of the surface. The somewhat arbitrary molecular areas were  $151 \text{ \AA}^2$  or  $9.12 \times 10^5 \text{ m}^2/\text{mol}$  for azocumene,  $201 \text{ \AA}^2$  or  $12.1 \times 10^5 \text{ m}^2/\text{mol}$  for BDPA (Koelsch's radical 1,1,3,3-bisdiphenylene-2-phenylallyl),  $109 \text{ \AA}^2$  or  $6.55 \times 10^5 \text{ m}^2/\text{mol}$  for azobenzene, and  $113 \text{ \AA}^2$  or  $6.78 \times 10^5 \text{ m}^2/\text{mol}$  for diphenyl nitroxide. A 0.02 monolayer fraction of azocumene on  $P_1H_1$  silica corresponds to 0.408 wt % of the silica.

**The Nature of the Material on the Silica.** It is important to distinguish between silica with crystals of the added organic compound and silica with the organic compound adsorbed on the surface. To ensure the latter state, most of our experiments were done with very small monolayer fractions, usually 0.02–0.04. There are several ways in which adsorption can be distinguished from silica plus crystals. First, the products from the adsorbed azocumene are notably different from those obtained from a melt. Second, the rate constants are lower than those in solution and increase with increasing  $C$ , leveling off at about 0.2–0.3 of a monolayer. It is only at 0.9 of a monolayer that we see a rate significantly above the plateau value, and then it is only 20% higher. Third is the behavior of BDPA put on by the same techniques. Exchange narrowing begins to affect the EPR spectrum at 0.0266 of a monolayer and above. At 0.09 monolayer fraction there is a superimposed sharp singlet indicating the presence of a population of radicals that are close together, though not necessarily in crystals. The mean distance between these large radicals at 0.09 monolayer fraction would be only about 30 Å if they were randomly distributed.

A fourth support for adsorption rather than crystallization is the absence of visible azocumene crystals or other anomalies in scanning electron micrographs of samples with  $C = 0.457$  at magnifications up to 135 000.

**Spectroscopy: EPR spectra** were taken with a Varian E-12 instrument using the X band ( $\sim 9$  GHz). The field marker on the Varian field/frequency lock accessory, and charred dextrose or DPPH, were used to measure the  $g$  values. Spectra were doubly integrated with an interfaced Varian 620i computer. Temperatures were controlled with an iron-constantan thermocouple. In variable temperature studies, the spectrum was obtained at a low temperature, then at a high temperature, and then again at a low temperature, to guard against pos-

**Table VI.** Chemical Shifts Downfield from Me<sub>4</sub>Si (ppm)

carbon	solution		on P <sub>0</sub> H <sub>1</sub> silica <sup>a-c</sup>
	CDCl <sub>3</sub>	CDCl <sub>3</sub> / CD <sub>3</sub> OD (1:1)	
methyl	26.83	25.83	31 ± 3 (263 Hz)
IV alkyl	71.81	72.40	77 ± 3 (150)
C <sub>1</sub> phenyl	145.70	145.59	151 ± 3
C <sub>2</sub> phenyl	126.35	125.63	
C <sub>3</sub> phenyl	126.69	126.06	135 ± 3 (463)
C <sub>4</sub> phenyl	128.35	127.64	

<sup>a</sup> At C = 0.457. <sup>b</sup> Line widths in parentheses. <sup>c</sup> Identical chemical shifts were observed on P<sub>1</sub>H<sub>1</sub> silica.

sible changes in the concentration of the radical during the measurements.

<sup>13</sup>C NMR of Adsorbed Compounds. These spectra were obtained with a Bruker 270 instrument. Our purpose was to examine the effect of adsorption and if possible to detect nonisolable intermediates such as the quinoidal dimers **8** and **9**, which should be present in photolyzed samples. Previous investigators<sup>23,25</sup> have found that adsorption broadens the lines 40–200 Hz and gives small shifts of –10 to +1.5 ppm relative to solution.

Cumene,  $\alpha$ -methylstyrene, dicumyl, azobenzene, and azocumene on P<sub>1</sub>H<sub>1</sub> or P<sub>0</sub>H<sub>1</sub> silicas at C = 0.176 to 0.50 all gave chemical shifts 3–11 ± 3 ppm further downfield from Me<sub>4</sub>Si than the solution values. The line widths ranged from 75 to 700 Hz and were greatest for dicumyl, azobenzene, and azocumene. These larger molecules may be oriented in a greater variety of ways to the irregular surface.

The chemical shifts for azocumene were compared with those in a hydroxylic solvent CDCl<sub>3</sub>/CD<sub>3</sub>OH as well as CDCl<sub>3</sub> (Table VI). The hydroxylic solvent gave small changes in the chemical shift and these were negative except for the methyl group, while the changes on silica were all positive. Apparently the hydroxylic solvent is not a good model for the effects of the silica surface.

The <sup>13</sup>C spectra of azocumene on silica after thermolysis or photolysis resembled the superposed spectra of the isolable products. Signals for quinonoid dimers, if present, could not be resolved from the others. These spectra were obtained without the benefit of magic angle spinning.

**Laser-Raman Spectra.** The instrument was a Cary 81 spectrometer with a Spectra Physics 125 helium–neon laser. The N=N stretch of azocumene was too weak to see in the crystal and was obscured by noise on the silica. Crystalline azobenzene gave bands at 1437 cm<sup>-1</sup> (trans) and 1470 (cis); on P<sub>1</sub>H<sub>1</sub> silica the bands were at 1440 and 1470 cm<sup>-1</sup>.

**Kinetics: Gas Evolution.** In each run, the nitrogen evolution was followed over the entire course of the reaction by using a single sample and a constant-volume, variable-pressure system.<sup>26</sup> Pressures were corrected for adsorbed nitrogen and for the small volume changes caused by the movement of the mercury in the manometer.

The silica sample was placed in a flask of accurately known volume and degassed in two stages, 1 h at 10<sup>-3</sup> mm and 10 h at 10<sup>-5</sup> to 10<sup>-6</sup> mm. This reaction vessel was then opened under argon, disconnected from its stopcock, and connected to the gas evolution apparatus, where it was again degassed overnight at 10<sup>-5</sup> mm before the run.

**UV Method.** This method used a different degassed and sealed ampule for each kinetic point. After the thermolysis the remaining azocumene was removed from the silica by washing with CHCl<sub>3</sub>, the solvent changed to *n*-hexane, and the amount of azocumene estimated from the UV spectrum.

**EPR Scavenger Method.** The azocumene and BDPA were adsorbed on the silica by using the SE technique for two adsorbates. Control samples of BDPA alone on the silica were also prepared by the SE technique. The samples, in EPR tubes fitted with a joint, were degassed in the usual way and stored at 0 °C in the dark until used.

A power saturation curve of the second integral of the derivative signal against (power)<sup>1/2</sup> was used to select operating conditions corresponding to the linear part of the function.

A series of spectra were then run for each kinetic point, consisting of a standard BDPA-on-silica sample to check and adjust the sensitivity, a control sample of BDPA alone on silica, and the kinetic sample being analyzed, in that order. This was repeated and the results of the double integration were averaged. Then the control and kinetic samples were placed in (or returned to) the thermolysis bath for varying lengths of time until the first derivative spectrum had decayed by a factor of two or more. Finally, the sample was heated long enough to obtain an infinity value. Concentrations were computed from the second integrals.

**Product Isolation and Analysis: Removal from the Surface.** Products were washed from the surface with 200–250 mL of CHCl<sub>3</sub> in small portions. A control in which the sample was subjected to a prolonged Soxhlet extraction produced no additional material.

**Characterization of Products.** After isolation by preparative GLC, the products were characterized by their proton NMR spectra, IR (for the low molecular weight products), low resolution mass spectra (for the high molecular weight products), and compared with synthetic samples.

The mixture of aromatized head-to-tail dimers **10** and **11** could not be readily separated and neither could it easily be prepared synthetically in pure form. The mixture was characterized by its <sup>1</sup>H and <sup>13</sup>C NMR and by low- and high-resolution mass spectra. The proportion of  $\alpha$ -ortho to  $\alpha$ -para isomers was approximately 3:1 on the basis of

**Table VII.** Azocumene Decomposition Rate Constants<sup>e</sup>

P <sub>0</sub> H <sub>1</sub>			P <sub>1</sub> H <sub>1</sub>		
C	T, °C <sup>g</sup>	k × 10 <sup>5</sup> , s <sup>-1</sup> <sup>f</sup>	C	T, °C <sup>g</sup>	k × 10 <sup>5</sup> , s <sup>-1</sup> <sup>f</sup>
0.0068	55.00	3.63 <sup>a,c</sup>	0.0089	54.97	4.47 <sup>a,c</sup>
0.0086	55.05	3.65 <sup>a,c</sup>	0.0101	55.03	4.37 <sup>a,c</sup>
0.0170	55.07	4.13 <sup>a,c</sup>	0.0204	55.25	4.75 <sup>a,c</sup>
0.0170	55.00	3.91 <sup>a,d</sup>	0.0492	54.97	4.85 <sup>b,c</sup>
0.0173	54.86	3.98 <sup>a,c</sup>	0.128	54.85	5.04 <sup>b,c</sup>
0.0455	54.96	4.16 <sup>b,c</sup>	0.249	54.98	5.24 <sup>b,c</sup>
0.0464	55.00	4.32 <sup>b,c</sup>	0.490	54.85	5.41 <sup>b,c</sup>
0.114	55.05	4.79 <sup>b,c</sup>	0.0186	65.12	19.0 <sup>a,c</sup>
0.228	55.00	4.79 <sup>b,c</sup>	0.0206	64.97	17.7 <sup>a,c</sup>
0.233	54.95	4.90 <sup>b,c</sup>	0.0188	35.10	0.251 <sup>a,d</sup>
0.455	54.82	5.01 <sup>b,c</sup>			
0.455	54.90	5.08 <sup>b,c</sup>	0.0166	P <sub>0</sub> H <sub>0</sub> 54.99	4.62 <sup>a,c</sup>
0.691	54.84	5.34 <sup>b,c</sup>	0.0444	55.03	5.26 <sup>b,c</sup>
0.901	54.82	6.17 <sup>b,c</sup>	0.228	55.00	5.40 <sup>b,c</sup>
0.0176	64.96	17.0 <sup>a,c</sup>	0.451	55.00	5.48 <sup>b,c</sup>
0.0180	64.74	16.2 <sup>a,c</sup>			
0.0193	34.90	0.218 <sup>a,d</sup>	0.0131	P <sub>1</sub> H <sub>0</sub> 55.06	4.81 <sup>a,c</sup>
0.0173	34.88	0.212 <sup>a,c</sup>	0.0496	54.87	5.64 <sup>b,c</sup>
			0.248	54.91	5.37 <sup>b,c</sup>
			0.468	54.84	5.51 <sup>b,c</sup>

<sup>a</sup> Adsorption technique SF. <sup>b</sup> Adsorption technique SE. <sup>c</sup> By gas evolution. <sup>d</sup> By UV. <sup>e</sup> See also Figure 4. <sup>f</sup> By gas evolution unless otherwise noted. <sup>g</sup> ± 0.15 °C.

the methyl  $^{13}\text{C}$  signals. The high-resolution molecular ion peak was at  $m/e$  238.1710, theoretical for  $\text{C}_{18}\text{H}_{22}$ , 238.1721.

The  $^{13}\text{C}$  lines for the quaternary carbons of **10** and **11** were not observed, due to the rapid pulse rate. Other lines were as follows. Isopropyl methyls:  $\alpha$ -ortho dimer  $\delta$  24.08 ppm (0.911 relative intensity),  $\alpha$ -para dimer 26.13 (0.323). Isopropylidene methyls:  $\alpha$ -ortho dimer 30.91 (1.000),  $\alpha$ -para 33.63 (0.307).  $\text{C}_6\text{H}_5$  rings in both  $\alpha$ -ortho and  $\alpha$ -para dimers: meta carbon 128.08 (0.316), ortho 125.18 (0.242), para 125.58 (0.528).  $\text{C}_6\text{H}_4$  ring in  $\alpha$ -ortho dimer: ortho to isopropyl 126.71 (0.912), meta to isopropyl 126.87 (1.000), para to isopropyl 128.00 (0.707), ortho to cumyl 126.04 (0.774).  $\text{C}_6\text{H}_4$  ring of  $\alpha$ -para dimer: ortho to isopropyl 127.03 (0.328), ortho to cumyl 126.04 (0.774). Note that the ortho-to-cumyl lines at  $\delta$  126.04 in the  $\alpha$ -ortho and  $\alpha$ -para dimers are not resolved.  $^1\text{H}$  NMR:  $\delta$  7.19 (aromatic multiplet, 9), 2.86 (septet, 1,  $J = 7.0$  Hz), 1.68 (singlet, 6), 1.24 (doublet, 6,  $J = 7.0$  Hz).

**Quantitative Product Determination.** The quantitative GLC analysis used a 10 ft  $\times$  0.25 in. column packed with 20% QF-1 on GasChrom P, 120–140 mesh, and a flame ionization detector. The inlet temperature was 205  $^\circ\text{C}$  and the detector temperature 290  $^\circ\text{C}$ . A column temperature of 85  $^\circ\text{C}$  was used for cumene and methylstyrene and 175  $^\circ\text{C}$  for the other products. The  $\text{N}_2$  flow rate was 180 mL/min. For GLC-mass spectrometry, a Varian Model 2700 chromatograph was interfaced with a Du Pont 491 mass spectrometer and a Hewlett-Packard 2100 Data System. The column, 4 ft  $\times$  0.25 in., was packed with 3% OV-1.

After washing the product from the surface, the solution was concentrated to 3–5 mL and an aliquot of the GLC standard was added. The sample was then transferred to a 25-mL flask and diluted to volume. The solution was then analyzed by GLC for cumene,  $\alpha$ -methylstyrene, and *p*-diisopropylbenzene (an internal standard), taking the result from three injections. The column temperature was then raised, high molecular weight compounds remaining from the previous injections were swept out, and the solution analyzed for biphenyl (internal standard) 1,1,3-trimethyl-3-phenylindan plus the aromatized head-to-tail dimers, and dicumyl, again taking the mean result from three injections. Calibration curves were used to relate the actual concentration of each component to that of its internal standard. The mixed peak of indan plus head-to-tail dimer was separated for purposes of identifying the components, but for routine quantitative determination it was analyzed by means of  $^1\text{H}$  NMR. On  $\text{P}_1$  silicas none of the indan is formed.

**Photolysis.** The light source was a high-power Hanovia UV lamp about 20 cm from the reaction vessel. The latter, a sealed tube made of fluted 51-mm Pyrex, was rotated about its long axis by a rotary evaporator drive during the photolysis to tumble the silica and ensure uniform exposure. The vessel was kept cool by a stream of tap water flowing over it. Irradiation time was ordinarily 96 h. Irradiation for 50 h decomposed 97% of the azocumene.

**Synthesis.** Azocumene **1** and azocumene- $d_6$  (**1- $d_6$** ) were made in best yields by the following route.

**Cumyl Azide.** This is a modification of a procedure used by Fowler to make another benzylic azide.<sup>27</sup> A suspension of 50.0 g (0.769 mol) of  $\text{NaN}_3$  in a solution of 300 g (1.836 mol) of  $\text{Cl}_3\text{CCOOH}$  in 300 mL of  $\text{CHCl}_3$  was prepared in a three-necked round-bottomed flask fitted with stirrer, dropping funnel and condenser. A solution of 65.5 g (0.554 mol) of  $\alpha$ -methylstyrene in 200 mL of  $\text{CHCl}_3$  was added dropwise with stirring at room temperature during 2 h, refluxed with stirring for 2 h, and then let stand overnight. It was then washed three times with  $\text{H}_2\text{O}$ , twice with aqueous  $\text{NaOH}$ , and twice with  $\text{H}_2\text{O}$ . The organic layer was dried over  $\text{MgSO}_4$  and concentrated in vacuo, and the crude oil used without further purification after it was found to have satisfactory IR and NMR spectra.

**Cumylamine.** A suspension of 25.0 g (0.659 mol) of 95%  $\text{LiAlH}_4$  in 200 mL of anhydrous ether was prepared in a similar apparatus, but with a drying tube added. The crude cumyl azide in 200 mL of anhydrous ether was added dropwise during 2 h to the chilled contents of the flask. It was then stirred for 1 h, refluxed with stirring for 4 h, then allowed to stand overnight. The reaction mixture was again chilled and treated with 120 mL of 20% aqueous  $\text{NaOH}$ , added dropwise with vigorous stirring. The layers were then separated, the ether layer was combined with an ether wash of the aqueous layer, and the combined ether layers were washed with water and then twice with dilute  $\text{HCl}$ . The aqueous  $\text{HCl}$  extract was then neutralized with dilute  $\text{NaOH}$ . The amine was taken up in ether, dried over  $\text{MgSO}_4$ , and concentrated. Vacuum distillation gave 46.1 g (0.341 mol, 61.5%

yield) of the pure amine, bp 45  $^\circ\text{C}$ , 1.0 mm (lit.<sup>28</sup> bp 72–73  $^\circ\text{C}$ , 8 mm). The IR and NMR spectra were identical with those of a sample made by the Hoffmann reaction.<sup>28</sup> The high-resolution mass spectrum showed a weak parent peak at  $m/e$  135.1052 (theory for  $\text{C}_9\text{H}_{13}\text{N}$ , 135.1057) and a  $\text{P} - 1$  peak at  $m/e$  134.0959 (theory 134.0969).

**Cumyl- $d_6$  Alcohol (1,1,1,3,3,3-Hexadeuterio-2-phenyl-2-propanol).** This was prepared by the procedure of Brown et al.<sup>29</sup> from hexadeuterioacetone (isotopic purity 99.5%). Vacuum distillation gave 71.1 g (0.501 mol, 80% yld), bp 75.0–75.5  $^\circ\text{C}$  (4 mm), mp 27–29  $^\circ\text{C}$  (lit.<sup>29</sup> bp 93  $^\circ\text{C}$  (11 mm), mp 30–31  $^\circ\text{C}$  for the nondeuterated alcohol). IR: 3350  $\text{cm}^{-1}$  (OH), 3065, 3040, and 3010 ( $=\text{C}-\text{H}$ ), 2240, 2135, 2080 (saturated  $\text{C}-\text{D}$ ). NMR:  $\delta$  7.33 (aromatic multiplet, 120), 2.52 (singlet, 23), and 1.44 (doublet, 1.5), which corresponds to 98.0% isotopic purity.

**Cumylamine- $d_6$ .** The synthesis of this amine from cumyl- $d_6$  alcohol was identical with the synthesis of the undeuterated amine via the azide. The IR spectrum of the azide showed absorption at 3070, 3040, 3010, 2240 (saturated  $\text{C}-\text{D}$ ), and 2120 ( $\text{N}_3$ ). Reduction with  $\text{LiAlH}_4$  gave the amine in 44.3% yield based on the alcohol: bp 74–75  $^\circ\text{C}$  (10 mm); IR 3320  $\text{cm}^{-1}$  and 3270 ( $\text{N}-\text{H}$ ), 3075, 3045, and 3015 ( $=\text{C}-\text{H}$ ), 2235, 2120, and 2090 (saturated  $\text{C}-\text{D}$ ), 1610 ( $\text{N}-\text{H}$ ), 1320, and 1285 ( $\text{C}(\text{CD}_3)_2$ ). NMR:  $\delta$  7.41 (aromatic multiplet, 159), 2.03 (singlet, 5), 1.84 (broad singlet, 57), indicating 98.0% deuterated methyl groups.

**$\alpha,\alpha$ -Dimethylbenzyl Isocyanate.** The procedure of Weinstock<sup>30</sup> for the modified Curtius reaction was used. To 4.5 g (0.027 mol) of  $\alpha,\alpha$ -dimethylphenylacetic acid in 100 mL of acetone in a 500-mL three-necked flask with condenser and addition funnel was added 10.0 mL of triethylamine. This mixture was cooled to  $-20$   $^\circ\text{C}$  and 4.5 mL (0.047 mol) of ethyl chloroformate dissolved in 10 mL of acetone was added dropwise with stirring, and then the mixture was stirred for 2 h at 10  $^\circ\text{C}$ . A solution of 5.0 g (0.077 mol) of  $\text{NaN}_3$  in 100 mL of  $\text{H}_2\text{O}$  was added dropwise with stirring over 30 min; then the solution was stirred for 6 h at 10  $^\circ\text{C}$ . The organic phase was taken up in *n*-pentane and washed with dilute  $\text{HCl}$  twice and then twice with dilute  $\text{Na}_2\text{CO}_3$ . After drying over  $\text{Na}_2\text{SO}_4$ , concentrating to an oil, and refluxing the oil with dry benzene (freshly distilled from  $\text{P}_2\text{O}_5$ ) for 4 h, the benzene was removed and the residue vacuum distilled: yield, 3.33 g (0.021 mol, 77.8%); bp 49.2  $^\circ\text{C}$  (0.65 mm) (lit. 44  $^\circ\text{C}$  at 0.75 mm,<sup>31</sup> 50–52  $^\circ\text{C}$  at 0.16 mm<sup>32</sup>); IR 3080, 3050, and 3020  $\text{cm}^{-1}$  ( $=\text{C}-\text{H}$ ), 2970, and 2925 (sat.  $\text{C}-\text{H}$ ), 2280 ( $-\text{N}=\text{C}-\text{O}$ ), 1395 and 1375 ( $\text{C}(\text{CH}_3)_2$ ); NMR  $\delta$  7.33 (aromatic multiplet, 5), 1.62 (singlet, 6). High-resolution mass spectrum: parent peak at  $m/e$  161.0830; theory for  $\text{C}_{10}\text{H}_{11}\text{NO}$  161.0840.

**Azocumene.** The procedure of Nelsen and Bartlett was used.<sup>1</sup> The yield from 13.5 g of cumylamine was 5.5 g (42%), mp 87.5–89.0  $^\circ\text{C}$  (lit.<sup>1</sup> 86.9–88.7  $^\circ\text{C}$ ). UV: max at  $\lambda$  367.5 nm,  $\epsilon$  44.5 in *n*-hexane (lit.<sup>1</sup>  $\lambda$  367,  $\epsilon$  44). IR: 3075, 3045, and 3010 ( $=\text{C}-\text{H}$ ), 2965, and 2920  $\text{cm}^{-1}$  (saturated  $\text{C}-\text{H}$ ), 1603 ( $\text{C}=\text{C}$ ), 1385, and 1369 ( $\text{C}(\text{CH}_3)_2$ ). NMR:  $\delta$  7.23 (aromatic multiplet, 5) 1.49 (singlet, 6).

**Cumylurea- $d_6$  ( $N^2,\alpha,\alpha$ -Dimethylbenzyl- $N^1-\alpha',\alpha'$ -di(perdeuteriomethyl)benzylurea).** To 2.83 g (0.018 mol) of freshly distilled  $\alpha,\alpha$ -dimethylbenzyl isocyanate in 15 mL of dry benzene (distilled from  $\text{P}_2\text{O}_5$ ) in a 50-mL, two-necked, pear-shaped flask was added at room temperature with stirring 2.70 g (0.020 mol) of cumylamine- $d_6$  in 10 mL of dry benzene. A white solid formed immediately. The reaction mixture was refluxed with stirring for 45 min and then allowed to stand overnight at room temperature. The solid was filtered out and washed with benzene: yield 5.15 g (0.017 mol, 94.5%), mp 225.5–227  $^\circ\text{C}$  (lit. mp 225–227<sup>31</sup> and 226–227  $^\circ\text{C}$ <sup>32</sup>). IR: 3315  $\text{cm}^{-1}$  ( $\text{N}-\text{H}$ ), 3075, 3045, and 3010 ( $=\text{C}-\text{H}$ ), 2960 and 2920 (saturated  $\text{C}-\text{H}$ ), 2240 (saturated  $\text{C}-\text{D}$ ), 1645 ( $\text{C}=\text{O}$ ), 1558 ( $\text{N}-\text{H}$ ), 1385 and 1367 ( $\text{C}(\text{CH}_3)_2$ ). NMR:  $\delta$  7.26 (aromatic multiplet, 88), 4.47 (singlet, 17.5), 1.51 (singlet, 54), indicating 98% ( $\text{CD}_3$ )<sub>2</sub>. High-resolution mass spectrum: parent  $m/e$  302.2277 (theory for  $\text{C}_{19}\text{H}_{18}\text{D}_6\text{N}_2\text{O}$ , 302.2264), and no peaks in the region of  $m/e$  296.

**Azocumene- $d_6$  (1- $d_6$ ).** This is a modification of the methods of Greene et al.<sup>33</sup> and Fowler.<sup>27</sup> Cumylurea- $d_6$ , 2.50 g (0.008 mol), was suspended in 100 mL of *tert*-butyl alcohol (freshly distilled from  $\text{Na}$ ) in a 500-mL flask screened from light. To the suspension was added dropwise during 5 min 4.0 mL (0.034 mol) of freshly prepared *tert*-butyl hypochlorite. The reaction mixture was stirred until all of the solid was gone (3 h). A freshly prepared solution of  $\text{K}^+ -\text{O}-t\text{-Bu}$  was added in *tert*-butyl alcohol, the mixture becoming warm. After stirring for 30 min at room temperature, the reaction mixture was poured into 200 mL of ice-water and extracted with *n*-pentane. The organic layer



was washed four times with water, dried over  $K_2CO_3$ , filtered, and concentrated at room temperature to a yellowish-green oil. On standing overnight in air, the oil formed crystals. These were filtered out and washed with *n*-hexane. Further concentration of the mother liquor yielded additional crystals. The combined crystalline material was recrystallized from dry ether, affording 0.55 g (0.002 mol, 25%), mp 86.5–88.0 °C (sealed capillary). IR: 3075, 3050, and 3015 ( $=C-H$ ), 2970, and 2920 (saturated  $C-H$ ), 2250 (saturated  $C-D$ ), 1603 ( $C=C$ ), 1385 and 1369 ( $C(CH_3)_2$ ). NMR:  $\delta$  7.37 (aromatic multiplet 100), 1.53 (singlet 52), indicating 98%  $(CD_3)_2$ . UV: max at 368.0 nm ( $\epsilon$  43.82).

**Acknowledgments.** This research was supported in part by Grant MPS73-04683 A01 from the National Science Foundation. Acknowledgment is made to the donors of the Petroleum Research Fund, administered by the American Chemical Society, for partial support of this research.

## References and Notes

- (1) S. F. Nelsen and P. D. Bartlett, *J. Am. Chem. Soc.*, **88**, 137 (1966).
- (2) S. F. Nelsen and P. D. Bartlett, *J. Am. Chem. Soc.*, **88**, 143 (1966).
- (3) W. A. Pryor and K. Smith, *J. Am. Chem. Soc.*, **92**, 5403 (1970).
- (4) See the Experimental Section for details.
- (5) G. J. Young, *J. Colloid Sci.*, **13**, 67 (1958).
- (6) A quantitative analysis of the data in terms of  $\tau_{rot}$  and  $\tau_{trans}$  was not attempted, since this laboratory is not equipped for accurate  $T_1$  and  $T_2$  measurements.
- (7) Koelsch's radical begins to decay at high temperatures. However, the decay and resulting decrease in concentration were shown not to be responsible for the increased resolution. The resolution was unchanged on running the temperature back down to 105 °C, obtaining a spectrum, raising the temperature to 180 °C, and again obtaining a spectrum.
- (8) (a) The spectra were recorded at a power level of 0.10 mW. The line width for diphenyl nitroxide adsorbed on silica is approximately 10 G. However, parameters for the calculation of  $\tau_{rot}$  from the nitroxide spectra have not been determined for this line width.<sup>8a</sup> The use of the value for a 3-G line width will probably cause  $\tau_{rot}$  to be overestimated. (b) S. A. Goldman, G. V. Bruno, and J. H. Freed, *J. Phys. Chem.*, **76**, 1858 (1972).
- (9) B. Loev and M. M. Goodman, "Progress in Separation and Purification", Vol. 3, E. S. Perry and G. J. Van Oss, Eds., Wiley, New York, 1970, pp 73–95.
- (10) T. Kawamura, A. Matsunami, T. Yonezawa, and K. Fukui, *Bull. Chem. Soc. Jpn.*, **38**, 1935 (1965).
- (11) J. E. Leffler and E. Grunwald, "Rates and Equilibria of Organic Reactions", Wiley, New York, 1963.
- (12) J. H. DeBoer and J. M. Vleeskens, *Proc. K. Ned. Akad. Wet., Ser. B*, **61**, 2 (1958).
- (13) J. B. Peri and A. L. Hensley, Jr., *J. Phys. Chem.*, **72**, 2926 (1968).
- (14) M. L. Hair, "Infrared Spectroscopy in Surface Chemistry", Marcel Dekker, New York, 1967.
- (15) (a) M. R. Basila, *J. Chem. Phys.*, **35**, 1151 (1961). (b) P. A. Leermakers, H. T. Thomas, L. D. Weis, and F. C. James, *J. Am. Chem. Soc.*, **88**, 5075 (1966).
- (16) (a) M. V. Kurashev, B. V. Romanouskii, and N. V. Kolesnichenko, *Neftekhimiya*, **17**, 507 (1977). (b) K. J. Skinner, R. J. Blaskiewica, and J. M. McBride, *Isr. J. Chem.*, **10**, 457 (1972); K. J. Skinner, H. A. Hochster, and J. M. McBride, *J. Am. Chem. Soc.*, **96**, 4698 (1974).
- (17) BDPA is stable at 55 °C on the pure silicas and decomposes only to the extent of 6–10% in ten or so azocumene half-lives on  $P_0$  silica. Galvinoxyl was too unstable, decreasing to zero concentration in 24 h. The spin trap nitrosobenzene on silica by itself generates a radical signal, presumably due to a nitroxide. *N*-tert-Butyl- $\alpha$ -phenylnitron<sup>18</sup> failed to trap any cumyl radicals.
- (18) E. G. Janzen, *Acc. Chem. Res.*, **4**, 31 (1971).
- (19) The central bond of the dicumyls is too weak to permit observation of the molecular ion. There is also a substantial isotope effect on the sensitivity of the mass spectrometric determination, with  $d_{12}$  considerably underestimated and  $d_6$  somewhat less so. Part of this error is cancelled in eq 9.
- (20) An analogous principle for rotations about bonds predicts that the greater the number of rotational potential energy minima, the lower the energy barrier.
- (21) At this fraction of an azobenzene monolayer a rough estimate of the average distance between azobenzene molecules is about 50 Å, or six times the diameter of a cumyl radical.
- (22) R. P. Bell, *Chem. Soc. Rev.*, **3**, 513 (1974).
- (23) I. D. Gay, *J. Phys. Chem.*, **78**, 38 (1974).
- (24) D. Geschke, W. D. Hoffmann, and D. Deininger, *Surf. Sci.*, **57**, 559 (1976).
- (25) D. Michel, *Surf. Sci.*, **42**, 453 (1974).
- (26) J. J. Zupancic, "Radical Reactions on Silica Surfaces: Azocumene," Dissertation, Florida State University, December 1978.
- (27) J. S. Fowler, *J. Org. Chem.*, **37**, 510 (1972).
- (28) A. C. Cope, T. T. Foster, and P. H. Towle, *J. Am. Chem. Soc.*, **71**, 3929 (1949).
- (29) H. C. Brown, J. D. Brady, M. Grayson, and W. H. Bonner, *J. Am. Chem. Soc.*, **79**, 1897 (1957).
- (30) J. Weinstock, *J. Org. Chem.*, **26**, 3511 (1961).
- (31) F. W. Hoover and H. S. Rothrock, *J. Org. Chem.*, **29**, 143 (1964).
- (32) A. Lambert, J. D. Rose, and B. C. L. Weedon, *J. Chem. Soc.*, 42 (1949).
- (33) F. D. Greene, J. C. Stowell, and W. R. Bergmark, *J. Org. Chem.*, **34**, 2263 (1969).

## Mechanism of Hydrolysis of Allenyl Acetates

Doris J. Scheffel, A. Randolph Cole, Dorothy M. Jung, and M. D. Schiavelli\*

Contribution from The Department of Chemistry,  
College of William and Mary, Williamsburg, Virginia 23185.  
Received May 18, 1979

**Abstract:** The acid-catalyzed hydrolyses of  $R_2C=C=CHOAc$  proceed by two mechanisms depending upon the degree of substitution at C-3. The monomethyl derivative exhibits acidity dependence, activation parameters, and a solvent isotope effect,  $k_{H_2O}/k_{D_2O} = 0.87$ , characteristic of normal ester hydrolysis, while the dimethyl derivative exhibits behavior characteristic of a slow proton transfer mechanism with  $k_{H_2O}/k_{D_2O} = 1.46$ . A study of  $\alpha$ - and  $\beta$ -secondary isotope effects in the hydrolysis of the dimethyl derivative strongly supports this conclusion. For this compound,  $k_H/k_{\alpha-D} = 1.00$  and  $k_H/k_{\beta,\delta_6} = 1.08$ .

The elegant work of Noyce and Pollack<sup>1,2</sup> has demonstrated that the acid-catalyzed hydrolysis of enol acetates such as ring-substituted  $\alpha$ -acetoxy styrenes, isopropenyl acetate, and vinyl acetate may proceed by two different pathways. At low acidities or when strongly electron-withdrawing substituents are present, a "normal" ester hydrolysis pathway is followed. Thus in 6%  $H_2SO_4$ , vinyl acetate and  $\alpha$ -acetoxy-*p*-nitrostyrene show solvent isotope effects,  $k_{H_2O}/k_{D_2O}$ , of 0.73 and 0.75, respectively. These effects strongly imply an equilibrium proton transfer mechanism is involved. In contrast, at higher acidities, each of these compounds shows a marked change in behavior with solvent isotope effects,  $k_{H_2O}/k_{D_2O}$ , being 2.69

(59%  $H_2SO_4$ ) for vinyl acetate and 3.25 (69%  $H_2SO_4$ ) for  $\alpha$ -acetoxy-*p*-nitrostyrene. These data imply a change in mechanism at higher acidity to one which involves slow proton transfer to carbon. Strong support for this conclusion was provided by a study of substituent effects in the  $\alpha$ -acetoxy styrenes where  $\rho = -1.9$  at  $H_0 = -2.6$ . Interestingly  $\alpha$ -acetoxy-*p*-methoxystyrene exhibits behavior suggestive of rate-limiting proton transfer at both low and high acidities. For this compound  $k_{H_2O}/k_{D_2O} = 2.50$ . More recent work by Tidwell et al.<sup>3</sup> and Loudon et al.<sup>4</sup> supports the earlier findings of Noyce and Pollack and further demonstrates the fine balance between the two mechanisms proposed.